Enhancing Axial Ratio Bandwidth of Dual Band Microstrip Patch Antenna for GSM Application

Pooja Sahoo, Pramod Kumar Singhal, and Karuna Markam

***Abstract*—This paper objective is to designed circular polarized microstrip patch antenna and enhances its axial ratio bandwidth. An antenna is designed using a stacking method. The design of the antenna is achieved by using two slots on the main radiating patch and one cross slot on the near field resonating parasitic patch (NFRP). The NFRP patch is positioned below the main radiating patch at some height. The main patch is called a modified Hilbert shaped antenna. A slots methodology on patches is used for the attainment of wider bandwidths. Improvement of the axial ratio bandwidth of an antenna is achieved by the introduction of NFRP patch. The antenna that has been designed resonated at frequencies 900 MHz and 1890 MHz, covering two bands, i.e. (725-990) MHz & (1800-1920) MHz with a return loss of -25 dB. Impedance bandwidths are obtained at 265 MHz and 120 MHz at these frequencies. Furthermore, (800–950) MHz and (1720-1920) MHz bands are covered by a 3-dB axial ratio. The percentage axial ratio bandwidths are obtained 17.14% and 10.98% over the operating bands. An average gain and radiation efficiency is reported 6.7 dBi and 84% for the antenna. The size of the antenna is calculated $0.36\lambda_0 \times 0.42\lambda_0 \times 0.042\lambda_0$. In summary the antenna is described as a dual-band, circular polarized with a stable gain and wider axial ratio bandwidth, deemed suitable for GSM (Global System for Mobile Communication) applications.**

Link to graphical and video abstracts, and to code: https://latamt.ieeer9.org/index.php/transactions/article/view/8610

***Index Terms* — Dual Band, NFRP patch, Microstrip patch antenna, Circular polarization, GSM**

I. Introduction

Circular polarization (CP) antennas are widely used in current communication systems such as radio frequency identification (RFID), global system for mobile communication (GSM), satellite and radar systems etc. Moreover, circular polarized antennas with small profile structures and lightweight radio apparatus are required. Microstrip patch antennas with compacted arrangement and ease of assimilation are repeatedly designed to create circular polarization. Various methodologies are reported for obtaining CP. CP radiation is produced in two orthogonal modes with equivalent amplitude and having 90° spatial phase shift [1]-[2]. A single-fed version [3]-[4] and a multi-fed version [1]-[5] methods are used for generating CP radiation in various patch antennas. In [6]-[7], a distributed patch and symmetric radiation pattern with stable near zenith coverage for GNSS is reported. Along with CP compact size of patch is also a requirement so symmetric slit and proximity feeding methods are used [8]-[9].

Multi-feed CP patches antennas have the advantages of wide impedance and axial ratio bandwidth [2]-[3]. However, heavy volumes or intricate structures are required for multi-fed CP antennas. CP Single-fed microstrip patch antennas have advantages of relatively lower developing costs and a compact design compared to multi-fed. Also a new design introduced for getting wider axial ratio i.e Koch fractal antenna for UHF RFID [10]-[11], circularly polarized laminated electromagnetic coupling patch antenna and its X-band sub-array in [12]. The act of the sub-array is enhanced with inline technology. Various types of microstrip patch antennas with improved polarized bandwidth are presented in [13]-[14]. Broad bandwidth has advantages in terms of deployment, cost reduction and flexibility. The microstrip patch antenna with broader bandwidth on band 848-926 MHz is presented in [15]. Additionally, space-based applications required a small and low-profile reader antenna configuration. All the above reported antennas are limited impedance bandwidths with narrow axial ratio.

However, CP antennas alone had a very narrow range, limiting its applications in general communications [16]-[17]. To meet a wide variety of polarized applications, adding an L-shaped plane on ground and a cut-out part of the direct feed layer, the axial ratio bandwidth of the reported antenna is increased by 16% [18]-[19]. However, the antennas in [20]-[21] needed a big ground plane, resulting in an antenna became bigger size.

For minimizing and controlling the size of the overall antenna, CP bandwidth is achieved by installing multiple generators with the same closest resonant frequency [22]-[23]. However, the result is a taller antenna. One of the promising ways to increase the CP bandwidth is a stacked structure. By correctly stacking numerous radiators with the same closest resonant frequencies a large operating bandwidth of an antenna can be achieved [24]-[25].

The elliptical hole added on patch [26], coupled rotated vertical metallic plates [27], serially coupled square slot ring [28] and ring on patches [29] are used to greatly improve the performance at the operating frequencies. CP antenna with improved axial ratio bandwidth is also used for the RFID applications [30]. In CP antennas, the axial ratio bandwidth improvement is a crucial task so a coin-shaped patch and a tape method are reported [31]-[32]. Recently a zero-order resonator with dual polarization on a compact patch antenna for GSM applications was proposed. The axial ratio bandwidth of that antenna found to be very less at operating band 2550 and 3850 MHz and having gain 3dBi [33]. Recently various circular polarized antennas for various applications of different shapes and sizes are proposed according to various improved parameters like high gain, directivity, multiband etc. [34]-[35]. Also many antennas are

Pooja Sahoo, P. K. Singhal, and Karuna Markam are with Madhav Institute of Technology and Science, Gwalior, M.P, India (e-mails: sahu.pooja2009@mitsgwalior.in, pks_65@mitsgwalior.in, and karuna_markam@mitsgwalior.in).

proposed for GSM application for a biomedical purpose and focusing on SAR value but that antennas are not circular polarized [36]-[37]. Most of the challenges are found in reported antennas that are limited axial ratio bandwidth over operating bands.

The work objective is to design a dual-band microstrip patch antenna with an improved axial ratio bandwidth. The axial ratio of a CP antenna measures the uniformity of its polarization at different angles. Maintaining a low axial ratio is important for good performance in circularly polarized antennas. In this paper a dual-band CP patch antenna with improved axial ratio bandwidth is proposed for GSM applications and covering frequency bands are 725-990 MHz and 1800-1920 MHz. The antenna is designed using a NFRP patch, a radiating square patch with two slots and a partially grounded plane.

On the NFRP patch, a cross slot is etched and placed below the main radiator with some height. The notched square patch is known as the hilbert curved patch [38] etched on the top substrate. Here the notched square patch with two slots and cuts are used for enhancing impedance bandwidths and it is called modified the hilbert shaped patch. A new pair orthogonal mode is generated by the NFRP patch in the near field, which produces a wider impedance bandwidth and an improved CP radiation. Section II presents the detailing of antenna structure.

The design process and the analysis of the parameters are presented in Section III. Result and analysis presentations are made in section IV. Section V presents the conclusion of the work. Assessment between the previously published antennas and proposed antenna is also presented in table IV.

II. ANTENNA GEOMETRY

Fig. 1 represents various configurations of the proposed antenna, which has three components: a modified square-shaped hilbert patch, a near-field resonant parasitic (NFRP) patch with cross-cut and a partially ground plane. Fig. 1(a) represents the side view of the antenna consisting of two patches; one is printed on top of the substrate-2 and another patch with cross grooves etched on substrate-1. NFRP patch is placed below the main radiating patch with some height *'h'*. For making the separation between two patches, uses small pieces of foam as a spacer at the corners.

The design antenna is connected to an SMA (sub-miniature version A) connector by threading the probe perpendicularly through the bottom substrate. The partially ground plane is used in this design. The 3D view of the antenna on CST is shown in Fig. 1(b), Fig. 1(c), and Fig. 1(d) represents the designing and dimension of a modified the hilbert shaped antenna and NFRP patch with a cross slot on it.

The antenna is designed and simulated using CST software. FR-4 substrate of thickness 1.6 mm is used for designing with the dielectric constant is 4.3 and loss tangent is 0.001. Table I provide a precise summary of the proposed antenna dimensions. Here '*X*' & '*Y*' are the length and width of the overall antenna. '*t*' & '*r*' define the width of the horizontal and vertical line on the NFRP patch as a cross slot. '*x*' & '*y*' are the length and width of the cross slot on the NFRP patch. '*L*' & '*W*' are the length and width of a square patch. '*L1*', '*L2*', '*L3*', '*L4*', '*W1*' & '*W2*' are the various lengths and widths defined in Fig. 1. The rest '*a*', '*b*', '*c*', '*d*', '*e*', '*f*' and '*g*' are slots parameters on the radiating patch.

TABLE I
PROPOSED DIMENSIONS OF REPORTED ANTENNA

Symbol	Value (mm)	Symbol	Value(mm)
X	80	***L***	70
Y	80	***L1***	34
t	4	***L2***	15
r	2	***L3***	15
x	40	***L4***	25
y	40	***W1***	15
W	70	***W2***	8
g	6	***c***	16
a	8	***d***	1
b	10	***e***	16
f	9	***h***	10

III. ANTENNA DESIGNING AND ANALYSIS

A. DESIGN PROCESS AND ANALYSIS

CST software is used to gradually model the antenna and for simulation. Design illustrations of the antenna shown in Fig. 2. Antenna_1 representing a Hilbert shaped antenna with one slot and getting one resonant band at 1870 MHz. Basically slots on radiating patches provide good return loss.

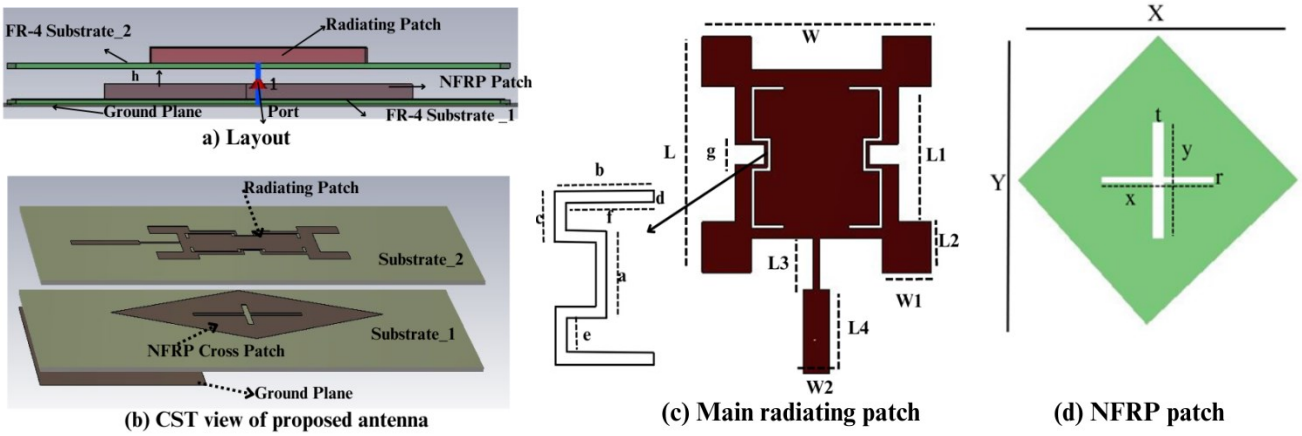

Fig. 1. Configurations of the proposed antenna (a) layout, (b) antenna designing on CST software, (c) Main radiating patch and (d) NFRP patch with slot.

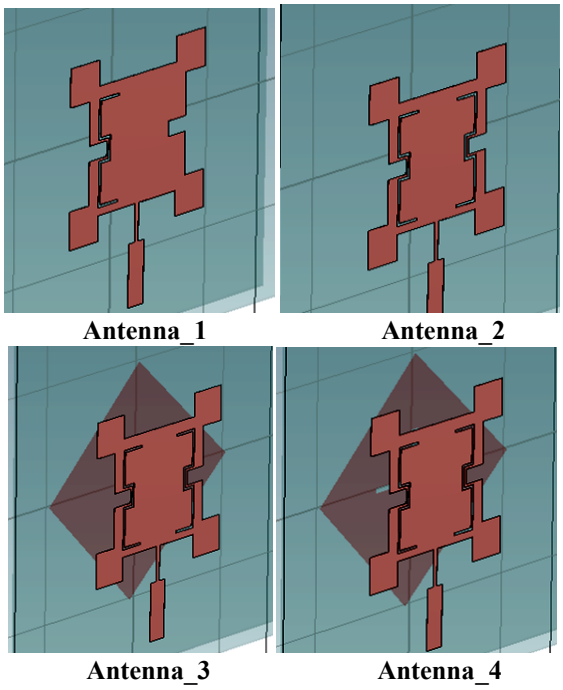

Fig. 2. Antenna Design iterations (a) main patch with one slot, (b) with two slots, (c) with NFRP patch, (d) with cross slot NFRP patch.

To maintain a compact structure and get a dual band, add one more slot on the patch as shown in antenna_2 and get one more additional resonant mode at 860 MHz along with 1870 MHz. Due to the two slots of equal length but opposite to each other on patch two resonant frequencies are generated. But the axial ratio is more than 3dB. Therefore, antenna_2 is linearly polarized. By adding more slots, frequencies are shifted and results are losing desired bands. Changing the polarization of antenna_2 from linear to circular introduced the concept of a near-field resonating patch below the main radiating patch. The NFRP patch is nothing but a radiating element that operates in the near field. Near field of any antenna refers to the region close to the radiating patch antenna, where the electromagnetic field properties are significantly different from those in the near field. The NFRP patch is not connected directly with the connector. It is only resonating in the field generated by antenna_2. After introducing the NFRP patch, the antenna axial ratio is found to be less than 3dB. Hence, antenna_3 is a dual-band circular polarized antenna.

The return loss coefficients of antennas step by step are shown in Fig. 3. The axial ratio (AR) bandwidth of antenna_3 is very narrow i.e. 6% and 9.2% on the frequency bands (860-910) MHz and (1.72-1.89) GHz. Axial ratio found below 3 dB at $\theta=10^0$ in xz plane and $\theta=11^0$ in yz plane at frequency 900 MHz. Similarly at frequency 1890 MHz, $\theta=15^0$ for xz plane and $\theta=14^0$ for yz plane is defined.

Now, for enhancing the AR bandwidth of antenna_3, one cross slot introducing on NFRP patch of thickness '*r*' (mm) and '*t*' (mm) called antenna_4. The cross slot is used to control the polarization and improve the axial ratio bandwidth of an antenna_3. The dimensions of the ground plane were not obtained by calculations but were chosen according to the most optimized size. After introducing the NFRP patch with a cross slot with partial ground plane, it is getting better bandwidth, i.e. 17% and 10.98% on operating band (725-990) MHz and (1800-1920) MHz. The axial ratio of antennas is shown in Fig. 4. From the graph it is clear that the antenna_4 (proposed) provides a wider impedance bandwidth and an enhanced axial ratio bandwidth.

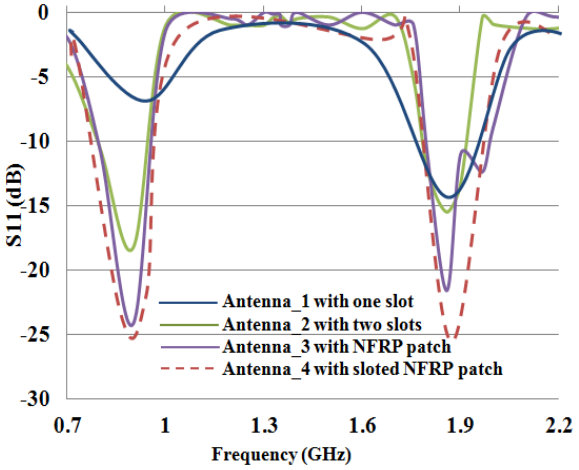

Fig. 3. S_{11} of antenna_1, antenna_2, antenna_3 and antenna_4.

Table II summarizes the results of all four antennas in terms of return loss S_{11} (dB), operating frequency bands, polarization and axial ratio. The antenna is circular polarized on both bands and the axial ratio covering bands are (800-950) MHz and (1720-1920) MHz. The influences of distance '*h*', thicknesses '*t*' and '*r*' of the cross slot on the NFRP patch are discussed in parametric study.

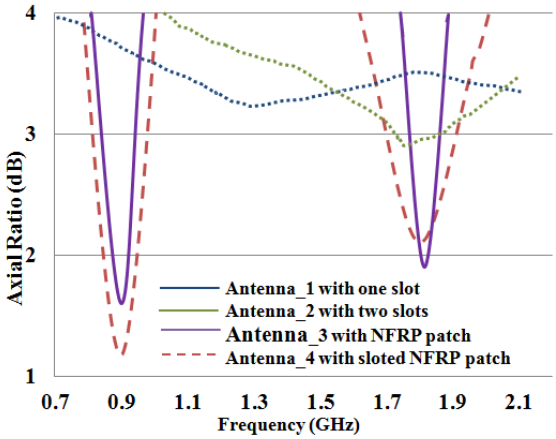

Fig. 4. Axial Ratio of antenna_1, antenna_2, antenna_3 and antenna_4.

TABLE II
SUMMARIZES OF ALL FOUR ANTENNA'S GRAPHICAL RESULTS

Antenna	S_{11} dB	Operating Bands (MHz)	F_r (MHz)	Polarization	Axial Ratio
Antenna_1	-12	(1750-1920)	1870	Linear	-
Antenna_2	-15	(800-940), (1800-1900)	860 & 1870	Linear	-
Antenna_3	-20	(800-950), (1800-1950)	860 & 1880	Circular	<3dB
Antenna_4	**-25**	**(725-990), (1800-1920)**	**900 & 1890**	**Circular**	**<3dB**

B. PARAMETRIC STUDY

Antenna_4 produces two circular polarized modes. In this section, describing the effect of *h* (distance) between the patches and influences in thickness of cross slots dimensions

on NFRP patch.

- Influence of *h*: - the separation (*h* mm) between the radiating patch and the NFRP patch of antenna_4 varying between 0 and 15 mm. After parametric analysis found the optimized solution at *h*=10mm and an improvement in axial ratio bandwidth. Fig. 5 and Fig. 6 show the graphical impact of '*h*' on return loss and axial ratio bandwidth on antenna_4. Table III summarizes the graphical results. At *h*=0mm, 5mm and 15mm, S_{11} is getting -12dB, -15dB and -22dB on operating bands. But at *h*=10 mm, it's getting better return loss S_{11}=-25dB on operating bands. Better return loss means efficient power transmitted with minimal signal loss.

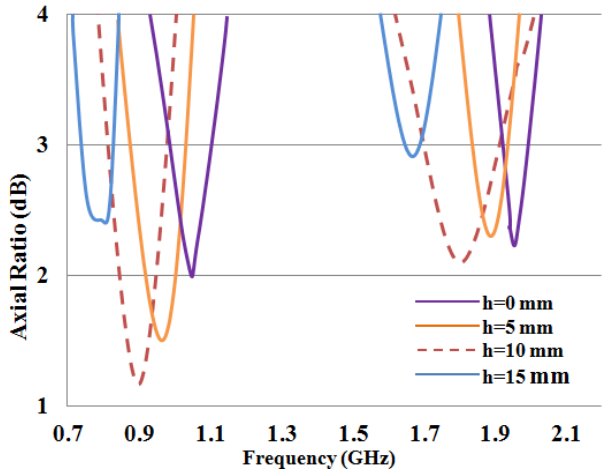

Fig. 5. Impact of '*h*' on axial ratio bandwidth antenna_4.

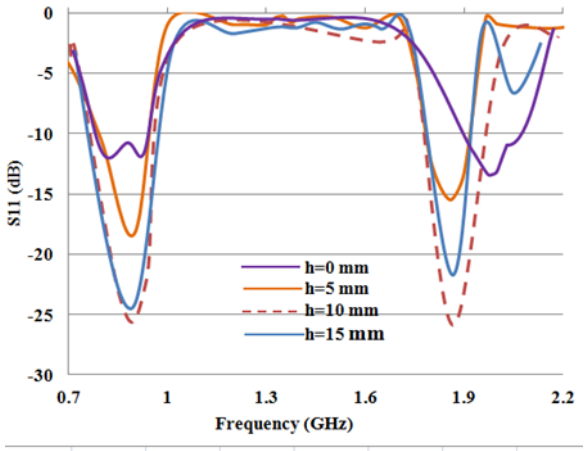

Fig. 6. impact of '*h*' on S_{11} (dB) of antenna_4.

TABLE III
SUMMARIZES IMPACT OF *h* (*mm*) ON PROPOSED ANTENNA_4

Distance '*h*'(*mm*)	S_{11} (dB)	Axial Ratio Bandwidth at 900 MHz (% BW)	Axial Ratio Bandwidth at 1.88 GHz (% BW)	Covering Bands (MHz)
0	-12	200 (19.04)	100 (5.12)	(950-1150), (1900-2000)
5	-15	100(10.5)	70 (3.71)	(900-1000), (1850-1920)
10	**-25**	**150(17.14)**	**200(10.98)**	**(800-950), (1720-1920)**
15	-22	80(10.2)	20(1.18)	(740-820), (1680-1700)

The axial ratio bandwidth also increases 17.14% at 900 MHz and 10.98% at 1880 MHz resonating frequencies shown in Table III. The axial ratio covering bands are (800-950) MHz and (1720-1920) MHz with enhanced impedance bandwidth 150 MHz and 200 MHz. The height '*h*' increasing continuously may cause a shifting resonance frequency and change the polarization. For many applications, the axial ratio is crucial, so need to carefully consider each optimized parameter.

- Variation in cross thickness '*t*' (mm) and '*r*' (mm) on NFRP patch:- variation in thickness *'t'* and '*r*' of cross slots on the NFRP patch are not too much impacted on return loss of antenna_4 as shown in Fig. 7, but improving radiation of the circular polarized antenna. AR bandwidths are changed and lead and lag operating bands with continuous variation in these parameters due to impedance mismatched between patches.

In summary, the cross slot thickness on the NFRP patch antenna determines its electrical properties in terms of variation in resonant frequency, impedance matching, bandwidth and polarization. Cross slots allow tuning the performance of the antenna to specific operational requirements. CST simulations are used to optimize the thickness of cross-slits to meet the desired antenna behaviour. It is found that return loss with enhanced impedance bandwidth is achieved at *r*=2mm and *t*=4mm as shown in Fig. 7.

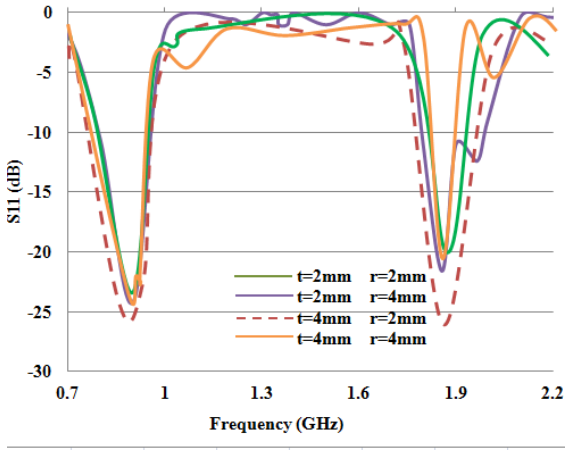

Fig. 7. Impact of thickness *'t' (mm)* and '*r' (mm)* on S_{11} (dB).

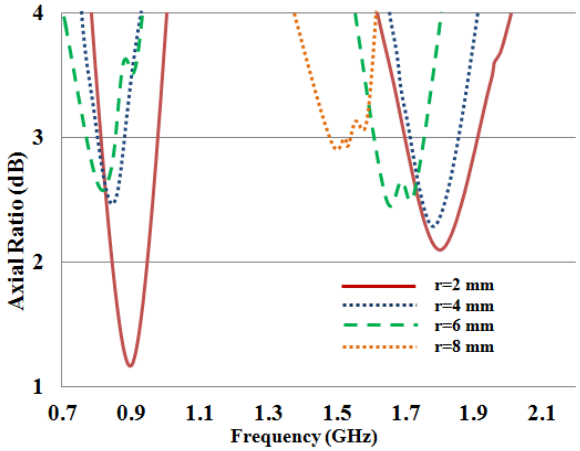

Fig. 8. Impact of '*r*' on axial ratio parameters when *t*=4mm.

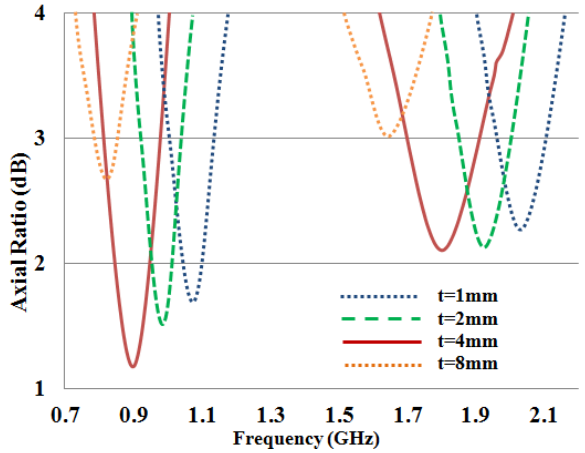

Fig. 9. Impact of *t* on axial ratio parameters when *r*= 2mm.

Similarly if *'r'* and *'t'* are increased continuously than result represent shift in resonant frequencies and lost axial ratio as shown in Fig. 8 and Fig. 9. This is happening due to the mismatching impedances between radiating patch and NFRP patch via wider slot, so the thickness of cross must be carefully evaluate. Table IV summarize the results of antenna_4 when the cross thickness is varying in term of *'t'* and '*r'*.

TABLE IV
SUMMARY OF NFRP CROSS THICKNESS VARIATION (t/r) mm ON AXIAL RATIO BANDWIDTH OF DESIGNED DUAL BAND ANTENNA

		r=2mm		
Axial Ratio(<3dB)	***t*=1mm**	***t*=2mm**	***t*=4mm**	***t*=8mm**
BW-1 (MHz)	150	150	270	Forbidden
BW-2 (MHz)	170	180	200	90
		***t*=4mm**		
Axial Ratio(<3dB)	***r*=2mm**	***r*=4mm**	***r*=6mm**	***r*=8mm**
BW-1 (MHz)	270	150	140	Forbidden
BW-2 (MHz)	200	100	100	Forbidden

IV. EXPERIMENTAL RESULTS AND DISCUSSIONS

An antenna_4 is designed and tested using a spectrum analyzer and antenna measurement system (AMS-A) to ensure its performance. The spectrum analyzer is configured to calculate the interference coefficient of an antenna and ANS setup is used for getting a radiation pattern. Measurement results are obtained in terms of AR bandwidth and impedance bandwidth. An antenna is operated at 900 MHz and 1880 MHz resonance frequencies. The covering bands are (725-990) MHz and (1800-1920) MHz with impedance bandwidth 175 MHz and 120 MHz. The axial ratio covering bands are (800-950) MHz and (1720-1920) MHz with bandwidth 150 MHz and 200 MHz for both bands. The percentage axial ratio bandwidths are enhanced by 17.14% and 10.98%. Fig. 10 presents measured and simulated values of the return loss. In case of $\Phi=90^0$, the direction of AR<3dB are obtained at $\theta=10^0$ & $\theta=11^0$ for lower band and $\theta=15^0$ & $\theta=14^0$ for upper band in xz and yz plane. Fig. 11 presents an axial ratio and gain of the prototype antenna. The maximum gain reported as 6.8dBi. The gains of the antenna determine the strength of the signal and effective coverage area. Fig. 12 and Fig. 13 representing the surface current density on the main radiating patch using without and with NFRP patch at 900 MHz and 1890 MHz frequencies. Which shows that maximum current density is accumulated near the patch by using NFRP patch and helps to control the electromagnetic waves.

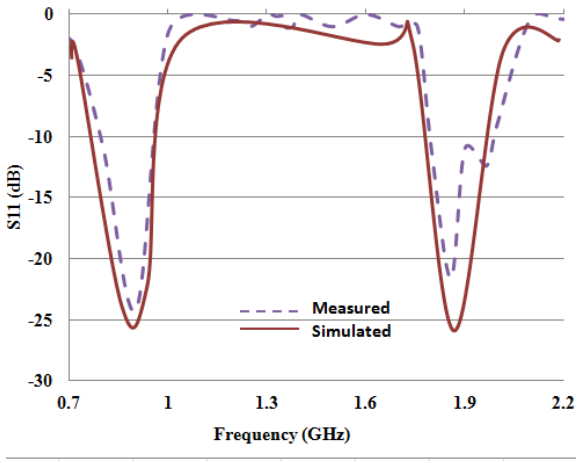

Fig. 10. Measured and simulated return loss of proposed antenna.

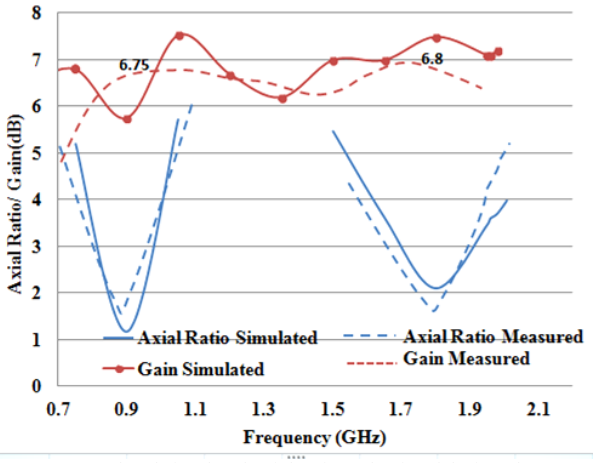

Fig. 11. Measured and simulated axial ratio and gain of designed antenna.

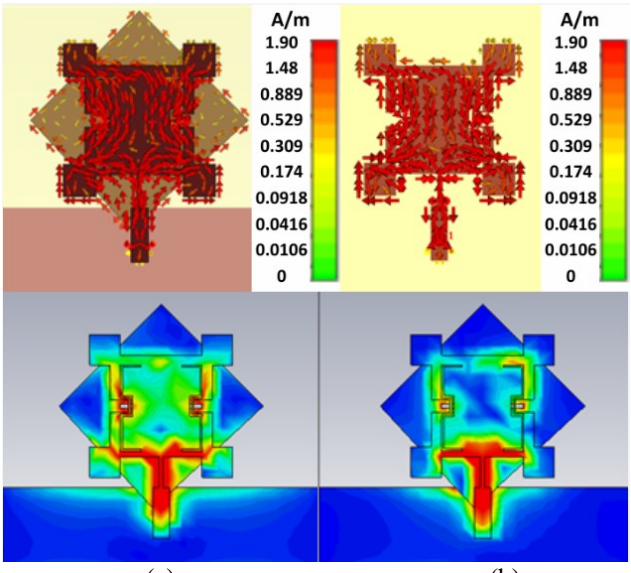

(a) (b)

Fig. 12. At 900 MHz, simulated surface current density of an antenna (a) with NFRP patch (b) without NFRP patch.

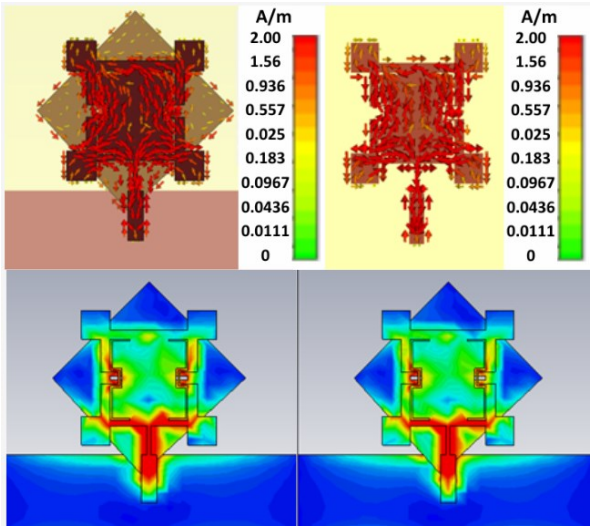

(a) (b)

Fig. 13. At 1890 MHz, simulated surface current density of an antenna (a) with NFRP patch (b) without NFRP patch.

In Fig. 14, the directivity of an antenna at resonant frequencies is presented. The directivity of an antenna focused on electromagnetic radiation in a specific direction, resulting in the maximum radiation found in a particular direction, i.e 6.65 dBi and 6.85 dBi at 900 MHz & 1800 MHz. Fig. 15(a) and 15(b) show the polar form of the radiation pattern. In polar form, the solid line presents the main lobe direction in E_{xz} plane when $\varphi=90^0$ and θ is varying. Similarly the dashed line is showing main lobe direction in E_{YZ} plane on different angle of θ^0. These patterns provide the information about antenna orientation, main lobe direction in term of directivity. The antenna is rotated at θ^0 from 0 to π and varying φ^0 from 0 to 2π.

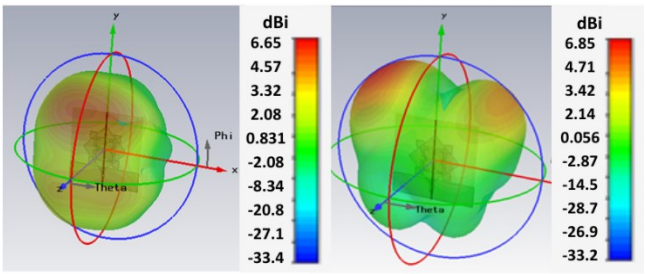

(a) (b)

Fig. 14. Simulated directivity of an antenna (a) 6.65dBi at 900 MHz and (b) 6.85dBi at 1890 MHz.

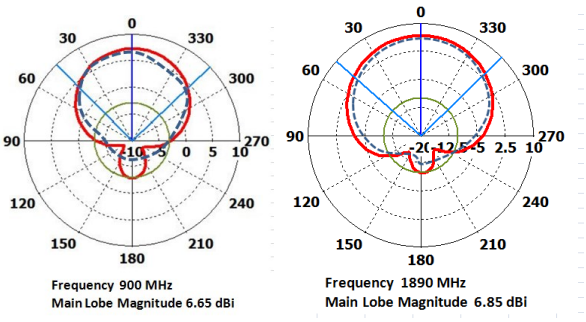

(a) *(b)*

Fig. 15. Radiation patterns of proposed antenna at frequency (a) 900 MHz, (b) 1890 MHz.

In CP antennas, both the planes are found approximately the same. The simulated radiation efficiency of dual band antenna is reported in Fig. 16. Average radiation efficiency is observed 84% shows how effectively power is transmitted.

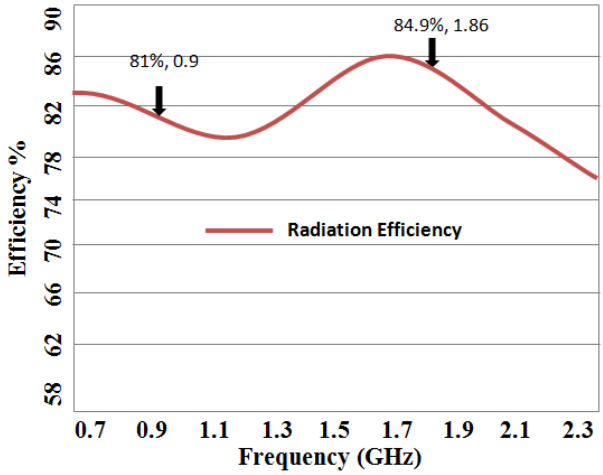

Fig. 16. Simulated radiation efficiency of proposed antenna.

Fig. 17 shows prototype views of an antenna and measurement setup. Designed antenna operates on two frequency bands, i.e. (800-950) MHz and (1720-1920) MHz. Axial ratio bandwidth also improved by 17.14% and 10.98%, which is twice the time the amount of reported axial ratio bandwidths in published papers as shown in table V. The size of the antenna is compact compared to others and the gain bandwidth is also enhanced. Justification of work is provided in Table V.

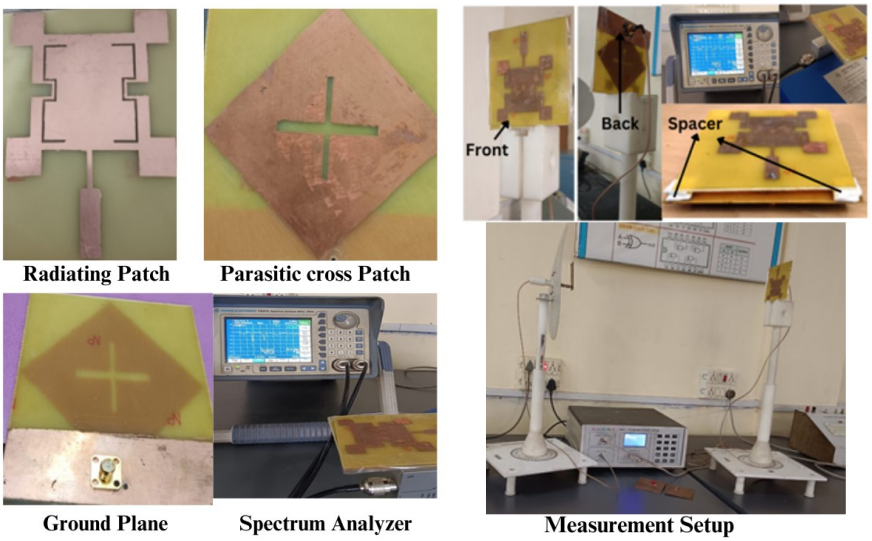

Fig. 17. Measurement Setup of modeled antenna.

TABLE V
COMPARISON OF RESULTS WITH PREVIOUS CP-GSM PUBLISHED PAPERS

Reference	AR covering Bands	Overlapping Bandwidth AR<3dB	Gain(dBi)	Dimension Size	Gain Bandwidth (Gain>6dBi)
[30]	846-926MHz	9%	7.3	$0.45\lambda_0\times0.45\lambda_0\times0.074\lambda_0$	15.0%
[24]	2390-2560MHz	6.94%	~7.0	$0.65\lambda_0\times0.65\lambda_0\times0.066\lambda_0$	/
[25]	1540-1620MHz	5.0%	6.5	$0.46\lambda_0\times0.46\lambda_0\times0.13\lambda_0$	/
[19]	865-946MHz	8.95%	7.0	$0.60\lambda_0\times0.60\lambda_0\times0.114\lambda_0$	/
[22]	902-929MHz	3.0%	6.0	$0.46\lambda_0\times0.46\lambda_0\times0.10\lambda_0$	/
[23]	901-930MHz	3.17%	7.0	$0.46\lambda_0\times0.46\lambda_0\times0.10\lambda_0$	/
[28]	2420-2640MHz	8.7%	7.0	$0.76\lambda_0\times0.76\lambda_0\times0.116\lambda_0$	12.2%
[29]	870–940 MHz	7.7%	7.0	$0.48\lambda_0\times0.48\lambda_0\times0.10\lambda_0$	13.6%
This Work	**(800-950)MHz**	17.14%	~6.85	$0.36\lambda_0\times0.42\lambda_0\times0.042\ \lambda_0$	17.1%
	(1720-1920)MHz	10.98%			

V. CONCLUSION

An improved axial ratio bandwidth, single-fed, dual band circular polarized patch antenna has been modeled and analyzed in this paper. The enhanced axial ratio bandwidth of microstrip patch antennas is important in situations where circular polarization must be maintained in the presence of multipath propagation, frequency variations, interference, or other difficult operating conditions. The parametric study provides better optimizing results for GSM applications. The modified patch antenna provided a dual-band at resonant frequencies 900 MHz and 1890 MHz. The NFRP patch changes the polarization from linear to circular and the cross slot on the NFRP patch provided a wider axial ratio bandwidth, which is the demand of wireless communication. The proposed antenna covering bands are (725-990) MHz and (1800-1920) MHz. Moreover, the 3-dB axial ratio covering bands are (800–950) MHz and (1720-1920) MHz. The percentage axial ratio of bandwidth is 17.14% and 10.98% achieved over the operating bands. Comparison provided that the designed antenna covers a wide dual-band with enhanced axial ratio bandwidth.

ACKNOWLEDGEMENT

The Author expresses deep gratitude to P. K. Singhal, Karuna Markam, and Yasho Vijay for their invaluable support and guidance, which were helpful in the successful completion of this work.

REFERENCES

[1] C. A. Balanis, "Microstrip Antennas" in *Antenna Theory: Analysis and Design*, 3rd ed., Hoboken, USA: John Wiley &Sons, 2005, pp. 859-864.

[2] Z. N. Chen, X. Qing, and H. L. Chung, "A universal UHF RFID reader antenna," *IEEE Trans. Microw. Theory Tech.*, vol. 57, no. 5, pp. 1275–1282, May. 2009. DOI: 10.1109/TMTT.2009.2017290

[3] Nasimuddin, Z. N. Chen, and X. Qing, "Asymmetric-Circular Shaped Slotted Microstrip Antennas for Circular Polarization and RFID Applications," *IEEE Trans. Antennas Propag.*, vol. 58, no. 12, pp. 3821-3828, Dec. 2010. DOI: 10.1109/TAP.2010.2078476

[4] Z. Wang, S. Fang, and S. Fu, and S. Jia, "Single-Fed Broadband Circularly Polarized Stacked Patch Antenna with Horizontally Meandered Strip for Universal UHF RFID Applications," *IEEE Trans. Microw. Theory Tech.*, vol. 59, no. 4, pp. 1066-1073, Apr. 2011. DOI: 10.1109/TMTT.2011.2114010

[5] K. L. Chung, Y. Li, and C. Zhang, "Broadband artistic antenna array composed of circularly-polarized Wang-shaped patch elements," *Int. J. Electron. Commun. (AEU)*, vol. 74, pp. 116-122, Apr. 2017. http://doi.org/10.1016/j.aeue.2017.02.006

[6] Q. Liu, J. Y. Shen, H. Liu, Y. Wu, M. Su, and Y. Liu, "Low-Cost Compact Circularly Polarized Directional Antenna for Universal UHF RFID Handheld Reader Applications," *IEEE Antennas Wireless Propag. Lett.*, vol. 14, pp. 1326-1329, 2015. DOI: 10.1109/LAWP.2015.2404033

[7] Q. Liu, Y. Li, Z. Mo, and Y. Liu, "Compact broadband circularly-polarised directional universal GNSS antenna with symmetric radiation pattern and stable near-zenith coverage," *IET Microw. Antennas Propag.*, vol. 11, no. 5, pp. 657-663, Apr. 2017. http://doi.org/10.1049/iet-map.2016.0815

[8] Nasimuddin, X. Qing, and Z. N. Chen, "Compact asymmetric-slit microstrip antennas for circular polarization," *IEEE Trans. Antennas Propag.*, vol. 59, no. 1, pp. 285–288, Jan. 2011. DOI: 10.1109/TAP.2010.2090468

[9] Y.-F. Lin, C.-H. Lee, S.-C. Pan, and H.-M. Chen, "Proximity-Fed Circularly Polarized Slotted Patch Antenna for RFID Handheld Reader," *IEEE Trans. Antennas Propag.*, vol. 61, no. 10, pp. 5283-5286, Oct. 2013. DOI: 10.1109/TAP.2013.2272677

[10] Z. N. Chen, X. Qing, and H. L. Chung, "A universal UHF RFID reader antenna," *IEEE Trans. Microw. Theory Tech.*, vol. 57, no. 5, pp. 1275–1282, May. 2009. DOI: 10.1109/TMTT.2009.2017290

[11] A. Farswan, A. K. Gautam, B. K. Kanaujia, and K. Rambabu "Design of Koch Fractal Circularly Polarized Antenna for Handheld UHF RFID Reader Applications," *IEEE Trans. Antennas Propag.*, vol. 64, no. 2, pp. 771-775, Feb. 2016. DOI: 10.1109/TAP.2015.2505001

[12] K. L. Chung and A. S. Mohan, "A circularly polarized stacked electromagnetically coupled patch antenna," *IEEE Trans. Antennas Propag.*, vol. 52, no. 5, pp. 1365-1369, May 2004. DOI: 10.1109/TAP.2004.827490

[13] K. L. Chung, "A Wideband Circularly Polarized H-Shaped Patch Antenna", *IEEE Trans. Antennas Propag.*, vol. 58, no. 10, pp. 3379-3383, Oct. 2010. DOI: 10.1109/TAP.2010.2055794

[14] C. Cho, H. Choo, and I. Park, "Broadband RFID tag antenna with quasi-isotropic radiation pattern," *Electron. Lett*., vol. 41, no. 20, pp. 1091-1092, 2005. DOI: 10.1049/el:20052337

[15] C. Cho, H. Choo, and I. Park, "Design of planar RFID tag antenna for metallic objects," *Electron. Lett.* vol. 44, no. 3, pp. 175-177, 2008. DOI: 10.1049/el:20083712

[16] K. Wei, J. Y. Li, L. Wang, R. Xu, and Z. J. Xing, "A New Technique to Design Circularly Polarized Microstrip Antenna by Fractal Defected Ground Structure," *IEEE Trans. Antennas Propag*., vol. 65, no. 7, pp. 3721-3725, Jul. 2017. DOI: 10.1109/TAP.2017.2700226

[17] J. M. Kovitz, H. Rajagopalan, and Y. Rahmat-Samii, "Circularly polarised half E-shaped patch antenna: a compact and fabrication-friendly design," *IET Microw. Antennas Propag.*, vol. 10, no. 9, pp. 932-938, Jun. 2016. https://doi.org/10.1049/iet-map.2015.0550

[18] C.-Y.-D. Sim, Y.-W. Hsu, and G. Yang, "Slits Loaded Circularly Polarized Universal UHF RFID Reader Antenna," *IEEE Antennas Wireless Propag. Lett.*, vol. 14, pp. 827–830, 2015. DOI: 10.1109/LAWP.2014.2382557

[19] C.-Y.-D. Sim, C.-C. Chen, R. Cao, B.-S. Chen, "A Circular Patch Antenna with Parasitic Element for UHF RFID Applications," *Int. J. RF Microw. Comput. -Aided Eng.*, vol. 25, no. 8, pp. 681-687, Oct. 2015. https://doi.org/10.1002/mmce.20905

[20] J. Zhuang, Y. Zhang, W. Hong, and Z. Hao, "A Broadband Circularly Polarized Patch Antenna with Improved Axial Ratio," *IEEE Antennas Wireless Propag. Lett.*, vol. 14, pp. 1180-1183, 2015. DOI: 10.1109/LAWP.2015.2396672

[21] M.-C. Tang, X. Chen, M. Li, and R. W. Ziolkowski, "A Bandwidth-Enhanced, Compact, Single-Feed, Low-Profile, Multilayered, Circularly Polarized Patch Antenna," *IEEE Antennas Wireless Propag. Lett.*, vol. 16, pp. 2258-2261, 2017. DOI: 10.1109/LAWP.2017.2713239

[22] C.-H.-Yeh, Y.-W. Hsu, and C.-Y.-D. Sim, "Equilateral Triangular Patch Antenna for UHF RFID Applications", *Int. J. RF Microw. Comput. -Aided Eng.*, vol. 24, no. 5, pp. 580-586, Mar. 2014. https://doi.org/10.1002/mmce.20801

[23] C.-Y.-D. Sim and C.-J. Chi, "A Slot Loaded Circularly Polarized Patch Antenna for UHF RFID Reader," *IEEE Trans. Antennas Propag.*, vol. 60, no. 10, pp. 4516-4521, Oct. 2012. doi.org/10.1049/iet-map.2017.0637

[24] C. Deng, X. Lv, and Z. Feng, "Low-profile circularly polarised patch–ring antenna with compact feeding network," *IET Microw. Antennas Propag.*, vol. 12, no. 3, pp. 410-415, Feb. 2018. doi.org/10.1049/iet-map.2017.0637

[25] T. Mondal, S. Samanta, R. Ghatak, and S. R. B. Chaudhuri, "A novel hexagonal wideband circularly polarized stacked patch microstrip antenna", *Microwave Opt. Technol. Lett.*, vol. 57, no. 11, pp. 2548-2554, Nov. 2015. https://doi.org/10.1002/mop.29383

[26] M.-C. Tang, X. Chen, M. Li, and R. W. Ziolkowski, "A Bandwidth-Enhanced, Compact, Single-Feed, Low-Profile, Multilayered, Circularly Polarized Patch Antenna," *IEEE Antennas Wireless Propag. Lett.*, vol. 16, pp. 2258-2261, 2017. DOI: 10.1109/LAWP.2017.2713239

[27] Y. M. Pan, W. J. Yang, S. Y. Zheng, and P. F. Hu, "Design of Wideband Circularly Polarized Antenna Using Coupled Rotated Vertical Metallic Plates," *IEEE Trans. Antennas Propag.*, vol. 66, no. 1, pp. 42-49, Jan. 2018. DOI: 10.1109/TAP.2017.2769690

[28] T.-N. Chang, J.-M. Lin, and Y. G. Chen, "A Circularly Polarized Ring-Antenna Fed by a Serially Coupled Square Slot-Ring," *IEEE Trans. Antennas Propag.*, vol. 60, no. 2, pp. 1132-1135, Feb. 2012. DOI: 10.1109/TAP.2011.2173138

[29] T.-N. Chang and J.-M. Lin, "Circularly Polarized Ring-Patch Antenna," *IEEE Antennas Wireless Propag. Lett.*, vol. 11, pp. 26-29, 2012. DOI: 10.1109/LAWP.2011.2182174

[30] J. Li, H. Liu, S. Zhang, M. Luo, Y. Zhang and S. He, "A Wideband Single-Fed, Circularly-Polarized Patch Antenna with Enhanced Axial Ratio Bandwidth for UHF RFID Reader Applications," in IEEE Access, vol. 6, pp. 55883-55892, 2018. DOI: 10.1109/ACCESS.2018.2872692

[31] X. Y. Liu, Y. Liu, and M. M. Tentzeris., "A Novel Circularly Polarized Antenna with Coin-Shaped Patches and a Ring-Shaped Strip for Worldwide UHF RFID Applications," *IEEE Antennas Wireless Propag. Lett.*, vol. 14, pp. 707–714, 2015. DOI: 10.1109/LAWP.2014.2378513

[32] J. Zhuang, Y. Zhang, W. Hong, and Z. Hao, "A Broadband Circularly Polarized Patch Antenna With Improved Axial Ratio," *IEEE Antennas Wireless Propag. Lett.*, vol. 14, pp. 1180-1183, 2015. DOI: 10.1109/LAWP.2015.2396672

[33] Rahimi M, et al. Design of compact patch antenna based on zeroth-order resonator for wireless and GSM applications with dual polarization. *Int J Electron Commun (AEÜ) (2014),* http://dx.doi.org/10.1016/j.aeue.2014.08.006

[34] Wang, Jinxiu, Yongzhi Cheng, Hui Luo, Fu Chen, and Ling Wu. "High-gain bidirectional radiative circularly polarized antenna based on focusing metasurface." *AEU-International Journal of Electronics and Communications* 151 (2022): 154222. https://doi.org/10.1016/j.aeue.2022.154222

[35] Kumar, A., Althuwayb, A. A., Chaturvedi, D., Kumar, R., & Ahmadfard, F. (2022). Compact planar magneto-electric dipole-like circularly polarized antenna. *IET Communications*, *16*(20), 2448-2453. https://doi.org/10.1049/cmu2.12499

[36] Chouhan, S., & Malviya, L. (2022, April). Stepped Patch Antenna for GSM Applications. In *2022 IEEE 11th International Conference on Communication Systems and Network Technologies (CSNT)* (pp. 72-75). IEEE. DOI: 10.1109/CSNT54456.2022.9787594

[37] Goswami, Sujit, Sujit Kumar Mandal, and Soumen Banerjee. "Compact Quad-Band Sickle-Shaped Monopole Antenna for GSM 900/WiMax/WLAN Applications." *Computers, Materials & Continua* 73.1 (2022). https://doi.org/10.32604/cmc.2022.025657

[38] K. J. Vinoy, K. A. Jose, V. K. Varadan and V. V. Varadan, "Hilbert curve fractal antennas with reconfigurable characteristics," *2001 IEEE MTT-S International Microwave Sympsoium Digest (Cat. No.01CH37157)*, Phoenix, AZ, USA, 2001, pp. 381-384 vol.1, doi: 10.1109/MWSYM.2001.966911

Pooja Sahoo is pursuing Ph.D. in Electronics Engineering from MITS, Gwalior, India. She did Master in engineering from MITS, RGPV Bhopal. She has published 15 papers in various national and international journals and IEEE conferences. Her research interests in the fields of Electronics and Antenna designing.

Dr. Pramod K. Singhal is a professor in the department of Electronics Engineering at MITS Gwalior M.P., India. He has more than 28 years teaching, research and development in diversified areas of Electronics Engineering. He has published 150 research papers in international and national journals and conferences including IEEE Transaction, SCI, ESCI, SCOPUS etc. His interest includes research and teaching in microwave engineering and RF antennas.

Dr. Karuna Markam is working as an assistant professor in the department of Electronics Engineering at MITS Gwalior M.P., India. She did M. Tech in Digital Communication from MANIT Bhopal and PhD from Barkatullah University Bhopal India. She has more than 20 years of teaching experience. She published more than 40 papers in various national and international journals and conferences in the field of Electronics.